Inorganic Chemistry

Article

pubs.acs.org/IC

2D and 3D Anilato-Based Heterometallic M(I)M(III) Lattices: The Missing Link

Samia Benmansour,* Cristina Vallés-García, Patricia Gómez-Claramunt, Guillermo Mínguez Espallargas, and Carlos J. Gómez-García*

Instituto de Ciencia Molecular (ICMol), Universidad de Valencia, C/Catedrático José Beltrán, 2, 46980 Paterna, Valencia, Spain

Supporting Information

ABSTRACT: The similar bis-bidentate coordination mode of oxalato and anilato-based ligands is exploited here to create the first examples of 2D and 3D heterometallic lattices based on anilato ligands combining M(I) and a M(III) ions, phases already observed with oxalato but unknown with anilato-type ligands. These lattices are prepared with alkaline metal ions and magnetic chiral tris(anilato)metalate molecular building blocks: $[M^{III}(C_6O_4X_2)_3]^{3-}$ (M^{III} = Fe and Cr; X = Cl and Br; $(C_6O_4X_2)^{2-}$ = dianion of the 3,6-disubstituted derivatives of 2,5-dihydroxy-1,4-benzoquinone, $H_4C_6O_4$). The new compounds include two very similar 2D lattices formulated as $(PBu_3Me)_2[NaCr(C_6O_4Br_2)_3]$ (**1**) and $(PPh_3Et)_2[KFe(C_6O_4Cl_2)_3](dmf)_2$ (**2**), both presenting hexagonal $[M^IM^{III}(C_6O_4X_2)_3]^{2-}$ honeycomb layers with $(PBu_3Me)^+$ in **1** or $(PPh_3Et)^+$ and dmf in **2** inserted between them. Minor modifications in the synthetic conditions yield the novel 3D lattice $(NEt_3Me)[Na(dmf)][NaFe(C_6O_4Cl_2)_3]$ (**3**), in which hexagonal layers analogous to **1** and **2** are interconnected through Na^+ cations, and $(NBu_3Me)_2[NaCr(C_6O_4Br_2)_3]$ (**4**), the first heterometallic 3D lattice based on anilato ligands. This compound presents two interlocked chiral 3D (10,3) lattices with opposite chiralities. Attempts to prepare **4** in larger quantities result in the 2D polymorph of compound **4** (**4′**). Magnetic properties of compounds **1**, **3**, and **4′** are reported, and in all cases we observe, as expected, paramagnetic behaviors that can be satisfactorily reproduced with simple monomer models including a zero field splitting (ZFS) of the corresponding S = 3/2 for Cr(III) in **1** and **4′** or S = 5/2 for Fe(III) in **3**.

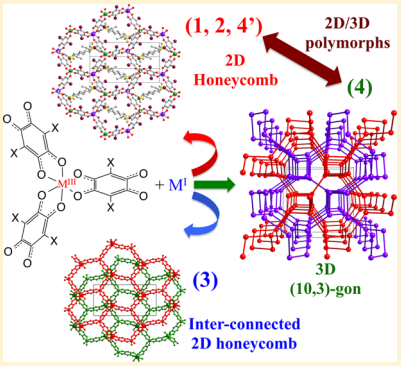

INTRODUCTION

Although crystal engineering of molecular materials is a relatively young discipline, it has already given rise to many materials designed and prepared with an appropriate choice of the precursor molecular building blocks. Some of them present useful physical properties such as long-range magnetic order (LRO),[1] spin crossover (SCO),[2] electrical conductivity and superconductivity (SC),[3] single molecule magnets (SMM),[4] or porosity,[5] to cite a few. Furthermore, crystal engineering has also provided very appealing examples of multifunctional materials where long-range magnetic order is combined with one or more interesting properties in a single molecular material. These examples include metallic ferromagnets,[6] magnetic conductors and superconductors,[7] chiral magnets[8,9] and conductors,[10,11] porous magnets,[12,13] magnets with SMM, etc.[14]

Most of these materials have been prepared by using well-known coordination chemistry tools: magnetic d- or f-block metal ions and simple anionic ligands as azide (N_3^-),[15,16] cyanide (CN^-),[17] dicyanamide ($N(CN)_2^-$),[18,19] and oxalato ($C_2O_4^{2-}$),[20] among others. The use of these simple ligands is based in (i) their ability to act as bridges affording polynuclear and extended complexes and (ii) their capacity to magnetically couple the metal ions they bridge. Among the above-mentioned ligands, oxalato is one of the most used ones in the last two decades. Its use was fuelled by the discovery made by Okawa et al.[20] of the family of 2D oxalato-based honeycomb lattices formulated as $[NBu_4][M^{II}M^{III}(C_2O_4)_3]$ (M^{II} = Mn, Fe, Co, Ni, and Cu; M^{III} = Cr and Fe) that present ordering temperatures in the range 6−48 K.[21,22] This family has been extended to include functional cations that impart metallic conductivity,[6,23] photochromism,[24] photoisomerism,[25] spin crossover,[26,27] chirality,[28,29] proton conductivity,[30] magnetic properties,[31−35] and nonlinear optical (NLO) properties.[36]

Although less numerous, these hexagonal layers have also been prepared combining M(I) with M(III) metal ions,[37−42] yielding paramagnetic molecular semiconductors, metals, and superconductors.[7,42,43]

Besides these honeycomb layers, the oxalato ligand has also been used to prepare heterometallic 3D chiral lattices. When all the metal centers in the $[MM'(C_2O_4)_3]^{n-}$ lattice possess the same chirality, the spatial disposition of the metals form a 3D structure with nonplanar rings of 10 metal atoms each connected to three different rings, i.e., (10,3) network. These 3D lattices were first observed for M(I)M(III) ions[44,45] and later were prepared for M(II)M(III) ions where, as expected, long-range ferro or ferrimagnetic order was observed.[46]

A topologically analogous ligand to oxalate is anilate (see Scheme 1), in which the central C═C moiety is changed by an

Received: February 24, 2015
Published: May 12, 2015

DOI: 10.1021/acs.inorgchem.5b00451
Inorg. Chem. 2015, 54, 5410−5418

Scheme 1. Bis-bidentate Coordination Mode of Oxalato, $dhbq^{2-}$, and the Anilate-Type Dianionic Ligands Used in This Work

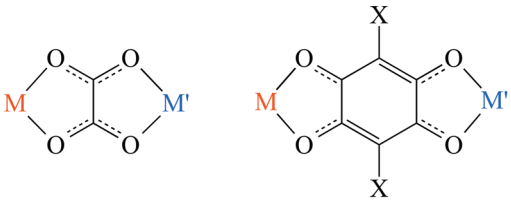

$(C_2O_4)^{2-}$ oxalato

X = H $(dhbq)^{2-}$

X = Cl or Br $(C_6O_4X_2)^{2-}$

aromatic ring. This ligand also promotes magnetic coupling[47−51] and thus can be used in the preparation of isoreticular magnetic networks to those reported for oxalate-based materials, with the advantage of tuning the ordering temperature through variation of the group X. In this sense, some of us have recently prepared a new family of heterometallic 2D honeycomb lattices that incorporates chirality and porosity to long-range magnetic order.[52]

Furthermore, very recently, these chiral, porous, and tunable 2D magnets have also proven to be able to host other functional cations as spin crossover ones,[53] further confirming the analogy with oxalate networks.

The similarity between the bis-bidentate coordination mode of oxalato and anilato-type ligands (see Scheme 1) prompted us to investigate the possibility to (i) prepare the 3D (10,3) chiral lattices obtained in the oxalato family and (ii) synthesize the M(I)M(III) 2D honeycomb lattices also observed in the oxalato series, two of the missing links in this oxalato−anilato analogy. This preparation constitutes a challenge in order to prove the ability of anilato-type ligands to build multifunctional materials, as previously done with the oxalato ligand, although with a higher degree of modularity because, as already shown in the M(II)M(III) 2D lattices,[52] the ordering temperatures of these lattices can be tuned by simply changing the X group in the anilato-based ligand.

An important drawback that needs to be overcome for the preparation of heterometallic anilato-based lattices is the presence of empty channels caused by the use of a larger linker.

With this aim, we present herein the first heterometallic anilato-based M(I)M(III) 2D lattices and the first heterometallic anilato-based 3D lattices, which represent the missing links in the oxalato−anilato analogy.

Compounds $(PBu_3Me)_2[NaCr(C_6O_4Br_2)_3]$ (**1**) and $(PPh_3Et)_2[KFe(C_6O_4Cl_2)_3](dmf)_2$ (**2**) form hexagonal 2D honeycomb lattices similar to the oxalato-based ones. Interestingly, compound **2** was obtained in a serendipitous way because the K^+ ions arise from impurities present in the recrystallization dmf solvent. Compound $(NEt_3Me)[Na(dmf)]$-$[NaFe(C_6O_4Cl_2)_3]$ (**3**) presents a novel 3D structure, not observed in the oxalato family, formed by hexagonal layers connected though interlayer Na^+ ions. Compound $(NBu_3Me)_2[NaCr(C_6O_4Br_2)_3]$ (**4**) presents the 3D heterometallic chiral (10,3) lattice already observed many times with oxalato ligands but never with anilato-type ligands, albeit, **4** contains two interpenetrated (10,3) chiral lattices with opposite chiralities, resulting in achiral crystals. This double lattice has no precedent in the oxalato-based 3D lattices because oxalato is much smaller than anilato. Interestingly, a second polymorph of compound **4**, denoted as **4′**, is obtained as a crystalline powder in the attempts to prepare **4** in large quantities. This compound is the 2D polymorph of compound **4**, and as far as we know, this 2D/3D polymorphism has never been observed in the oxalato families and shows the larger versatility of the anilato-type ligands compared to the oxalato one.

EXPERIMENTAL SECTION

Materials and Methods. *N,N*-Dimethylformamide (dmf), dichloromethane (CH_2Cl_2), tributylmethylfosfonium methylsulfate $(PBu_3Me)(CH_3OSO_3)$, triphenylethylfosfonium bromide $(PPh_3Et)Br$, triethylmethylammonium chloride $(NEt_3Me)Cl$, tributylmethylammonium chloride $(NBu_3Me)Cl$, NaOH, KOH, chloranilic acid ($H_2C_6O_4Cl_2$), bromanilic acid ($H_2C_6O_4Br_2$), and the metal chloride salts $FeCl_3·6H_2O$ and $CrCl_3·6H_2O$ are commercially available and were used as received without further purification.

*Synthesis of $(PBu_3Me)_2[NaCr(C_6O_4Br_2)_3]$ (**1**).* A solution of $CrCl_3·6H_2O$ (213 mg, 0.8 mmol) in H_2O (5 mL) was added dropwise to an aqueous solution (50 mL) containing 715 mg (2.4 mmol) of $H_2C_6O_4Br_2$, 192 mg (4.8 mmol) of NaOH and 780 mg (2.4 mmol) of $(PBu_3Me)(CH_3OSO_3)$. The resulting solution was heated at 60 °C for 30 min and then cooled to room temperature, resulting in the formation of a violet precipitate. This solution was extracted with three portions of CH_2Cl_2 (50 mL each). The resulting deep-red lower CH_2Cl_2 fractions were collected, and the solvent was removed by rotary evaporation. The obtained deep-red lacquer solid was recrystallized with *N,N*-dimethylformamide (dmf) to afford **1** as red elongated octahedral crystals after slow evaporation of the solvent (166 mg, yield 15%). Elemental Anal. Calcd for $C_{44}H_{60}Br_6O_{12}P_2CrNa$ (M_w = 1397.31): C, 37.82; H, 4.33. Found: C, 37.88; H, 4.16. The elemental ratio estimated by electron probe microanalysis (EPMA): Br/P/Cr/Na = 6.0/2.1/1.0/0.9 agrees with the calculated one (6/2/1/1) from the proposed formula. FT-IR (ν_{max}/cm^{-1}, KBr pellet): 3428(s), 3130(m), 2958(m), 2930(m), 2871(m), 1644(m), 1521(s), 1402(m), 1346(s), 1302(m), 985(m), 932(m), 809(m), 603(m), 559(m), 503(m), 408(m). The phase purity of this compound was confirmed by powder X-ray diffraction analysis (see Supporting Information).

*Synthesis of $(PPh_3Et)_2[KFe(C_6O_4Cl_2)_3](dmf)_2$ (**2**).* This compound was prepared by a similar method to **1** but using $FeCl_3·6H_2O$ (0.216 mg, 0.8 mmol) instead of $CrCl_3·6H_2O$, $H_2C_6O_4Cl_2$ (500 mg, 2.4 mmol) instead of $H_2C_6O_4Br_2$ and $(PPh_3Et)Br$ (891 mg, 2.5 mmol) instead of $(PBu_3Me)(CH_3OSO_3)$. The main difference is that compound **2** is obtained from the aqueous phase that is also evaporated and recrystallized from dmf to obtain violet hexagonal plate-like crystals (major phase) and a few red hexagonal prismatic crystals after slow evaporation of the solvent. Because only the hexagonal prisms give good reflections, we could only determine the structure of this minor phase. The elemental ratio estimated by electron probe microanalysis (EPMA): Cl/P/Fe/K = 6.0/2.0/1.1/1.1 agrees with the calculated one (6/2/1/1) from the proposed formula. The major phase shows an elemental analysis compatible with the formula $(PPh_3Et)_3[Fe(C_6O_4Cl_2)_3]$ corresponding to a monomeric phase. The K^+ ions present in compound **2** originate from K^+ impurities present in the dmf solvent used (this presence was confirmed by electrospray mass spectroscopy of the solvent).

*Synthesis of $(NEt_3Me)[Na(dmf)][NaFe(C_6O_4Cl_2)_3]$ (**3**).* A solution of $FeCl_3·6H_2O$ (216 mg, 0.8 mmol) in H_2O (5 mL) was added dropwise to an aqueous solution (50 mL) containing 500 mg (2.4 mmol) of $H_2C_6O_4Cl_2$, 192 mg (4.8 mmol) of NaOH and 364 mg (2.4 mmol) of $(NEt_3Me)Cl$. The resulting solution was heated at 60 °C for 30 min and then cooled to room temperature, resulting in the formation of a violet precipitate. Because the addition of CH_2Cl_2 did not resulted in the separation of two phases, the solution was rotoevaporated and the resulting dark-violet solid was dissolved in 25 mL of dmf to afford **3** as purple prismatic single crystals after slow evaporation of the solvent (472 mg, yield 65%). Elemental Anal. Calcd for $C_{28}H_{25}Cl_6O_{13}N_2FeNa_2$ (M_w = 912.03): C, 36.87; H, 2.76; N, 3.07. Found: C, 35.73; H, 2.24; N 3.10. The elemental ratio estimated by

DOI: 10.1021/acs.inorgchem.5b00451
Inorg. Chem. 2015, 54, 5410−5418

Table 1. Crystallographic Data for Compounds 1−4

compd	1	2	3	4
empirical formula	$C_{44}H_{60}Br_6O_{12}$ P_2CrNa	$C_{64}H_{54}Cl_6O_{14}$ N_2P_2FeK	$C_{28}H_{25}Cl_6O_{13}$ N_2FeNa_2	$C_{44}H_{60}Br_6O_{12}$ N_2CrNa
fw	1397.31	1444.68	912.03	1363.39
cryst color	red	red	purple	purple
cryst size	0.16 × 0.12 × 0.10	0.14 × 0.07 × 0.04	0.10 × 0.06 × 0.04	0.17 × 0.14 × 0.07
temp (K)	120(2)	120(2)	120(2)	120(2)
wavelength (Å)	0.71073	0.71073	0.71073	0.71073
cryst syst, Z	monoclinic, 2	monoclinic, 2	monoclinic, 4	cubic, 8
space group	$P2_1$	$P2_1$	$P2_1/c$	$I\bar{4}3d$
a (Å)	9.8809(4)	9.7327(3)	12.7905(3)	22.4250(9)
b (Å)	23.8659(8)	24.9615(7)	25.9152(6)	22.4250(9)
c (Å)	12.4131(4)	13.3675(4)	10.6329(2)	22.4250(9)
α (deg)	90	90	90	90
β (deg)	104.868(4)	108.147(4)	92.472(2)	90
γ (deg)	90	90	90	90
V (Å^3)	2829.21(17)	3086.01(16)	3521.19(13)	11277.1(8)
ρ_{calc} (Mg/m^3)	1.640	1.555	1.720	1.606
μ(Mo Kα) (mm^{-1})	4.556	0.693	0.976	4.517
θ range (deg)	3.07−25.03	2.93−29.63	2.90−29.98	2.87−25.09
reflns collected	35207	48660	58047	148006
independent reflns (R_{int})	9979 (0.0412)	14861 (0.0473)	9582 (0.0522)	1679 (0.1582)
reflns used in refinement, n	9979	14861	9582	1679
LS parameters, p/ restraints, r	604/2	818/1	462/14	103/0
$R1(F)$,[a] $I > 2\sigma(I)$	0.0326	0.0579	0.0413	0.0633
$wR_2(F^2)$,[b] all data	0.0758	0.1620	0.1076	0.1729
$S(F^2)$,[c] all data	1.043	1.016	1.031	1.123

[a] $R_1(F) = \sum||F_o| - |F_c||/\sum|F_o|$. [b] $wR_2(F^2) = [\sum w(F_o^2 - F_c^2)^2/\sum wF_o^4]^{1/2}$. [c] $S(F^2) = [\sum w(F_o^2 - F_c^2)^2/(n + r - p)]^{1/2}$.

electron probe microanalysis (EPMA): Cl/Fe/Na = 6.0/1.0/2.2 agrees with the calculated one (6/1/2) from the proposed formula. FT-IR (ν_{max}/cm^{-1}, KBr pellet): 3440(s), 3141(m), 1633(m), 1524(s), 1399(m), 1361(s), 1332(m), 1141(m), 1000(m), 847(m), 605(m), 577(m), 508(m). The phase purity of this compound was confirmed by powder X-ray diffraction analysis (see Supporting Information).

Synthesis of $(NBu_3Me)_2[NaCr(C_6O_4Br_2)_3]$ (4). A solution of $CrCl_3\cdot 6H_2O$ (213 mg, 0.8 mmol) in H_2O (5 mL) was added dropwise to an aqueous solution (50 mL) containing 715 mg (2.4 mmol) of $H_2C_6O_4Br_2$, 192 mg (4.8 mmol) of NaOH and 566 mg (2.4 mmol) of $(NBu_3Me)Cl$. The resulting solution was heated at 60 °C for 30 min and then cooled to room temperature, resulting in the formation of a violet precipitate. This solution was dried by rotary evaporation, and the resulting dark-violet solid was stirred with 50 mL of absolute EtOH during 24 h and then filtered. The solid obtained (i.e., the fraction nonsoluble in EtOH) was dissolved in dmf to afford **4** as purple prismatic single crystals (minor phase) mixed with a burgundy crystalline powder (major phase, compound **4′**) after slow evaporation of the solvent. For **4**, the elemental ratio estimated by electron probe microanalysis (EPMA): Br/Cr/Na = 6.0/1.2/1.0 agrees with the calculated one (6/1/1) from the proposed formula. The powder X-ray diffractogram of the major phase (**4′**) strongly suggests that it has the same 2D structure that compounds **1** and **2** (see Supporting Information). Elemental Anal. Calcd for **4′**: $C_{44}H_{60}Br_6O_{12}N_2CrNa$ (M_w = 1363.39): C, 38.76; H, 4.44; N, 2.06. Found: C, 38.87; H, 4.21; N 2.68. For **4′**, the elemental ratio estimated by electron probe microanalysis (EPMA): Br/Cr/Na = 6.0/1.2/1.0 agrees with the calculated one (6/1/1) from the proposed formula.

Structural Characterization of Compounds 1−4. Single crystals of compounds **1**−**4** were mounted on glass fibers using a viscous hydrocarbon oil to coat the crystals and then transferred directly to the cold nitrogen stream for data collection. X-ray data were collected at 120 K on a Supernova diffractometer equipped with a graphite-monochromated Enhance (Mo) X-ray source (λ = 0.71073 Å). The program CrysAlisPro, Oxford Diffraction Ltd., was used for unit cell determinations and data reduction. Empirical absorption correction was performed using spherical harmonics, implemented in the SCALE3 ABSPACK scaling algorithm. Crystal structures were solved and refined against all F^2 values using the SHELXTL suite of programs.[66] Non-hydrogen atoms were refined anisotropically (when no disorder was present), and hydrogen atoms were assigned fixed isotropic displacement parameters. Hydrogen atoms of the aromatic rings were placed in calculated positions and were refined using idealized geometries (riding model). Compound **2** is a twin crystal with two major components, but the detwinned data could not be used due to low completeness (ca. 70%). The possible presence of an inversion center in **2** (with a change of space group from $P2_1$ to $P2_1/n$) has been rejected as solution in $P2_1/n$ causes the appearance of disorder in the anilato ligand and inconsistent anisotropic thermal displacements. Furthermore, **2** is isoreticular to **1**, which clearly belongs to the $P2_1$ space group. The triethylmethylamonium cation in **3** has been modeled with disorder over two positions with occupancies 53.3(7):46.7(7). The Cr and Na centers appear disordered in the metallic positions in **4** with 50% occupancy each. A summary of the data collection and structure refinements is provided in Table 1.

Powder X-ray Diffraction. The X-ray powder diffractograms were collected for polycrystalline samples of compounds **1**, **3**, and **4′** using a 0.5 mm glass capillary that was mounted and aligned on a Empyrean PANalytical powder diffractometer, using Cu Kα radiation (λ = 1.54177 Å). A total of 2 scans were collected at room temperature in the 2θ range 2−60°. Pawley refinements[67] were performed using the TOPAS computer program[68] and revealed an excellent fit to a one-phase model for compounds **1** (R_{wp} = 0.0256; GOF = 1.781; Figure S1, Supporting Information), **3** (R_{wp} = 0.0162; GOF = 1.278; Figure S2, Supporting Information), and **4′** (R_{wp} = 0.0323; GOF = 2.420; Figure S3, Supporting Information), indicating the absence of any other detectable crystalline phases. In all cases, the unit cell obtained from the Pawley refinement is consistent with those obtained by single-crystal diffraction (see the Supporting Information).

Physical Properties. FT-IR spectra were performed on KBr pellets and collected with a Nexus-Nicolet 5700 spectrophotometer. Elemental C, H, N analyses were performed with a CE instrument EA 1110 CHNS analyzer. The X:M^{III}:M^{I}:P ratios of the bulk samples were estimated by electron probe microanalysis (EPMA) performed in a

DOI: 10.1021/acs.inorgchem.5b00451
Inorg. Chem. 2015, 54, 5410−5418

Philips SEM XL30 equipped with an EDAX DX-4 microprobe. Magnetic measurements were performed with a Quantum Design MPMS-XL-5 (or XL-7 for **4′**) SQUID magnetometer in the 2−300 K temperature range with applied magnetic fields of 0.1 T for **3** and **4′** and 0.5 T for **1** on polycrystalline samples of compounds **1**, **3**, and **4′** (with masses of 3.45, 9.99, and 9.78 mg, respectively). Isothermal magnetization measurements were performed at 2 K with magnetic fields of up to 5 T (7 T for **4′**). Susceptibility data were corrected for the sample holder and for the diamagnetic contribution of the salts using Pascal's constants.[69]

RESULTS AND DISCUSSION

Synthesis. The synthesis of all the compounds was performed following a one-pot reaction between the corresponding M(III) chloride with an aqueous solution containing a bulky cation and the deprotonated anilate-type dianion. This last is obtained by adding NaOH to the corresponding chloranilic, $H_2C_6O_4Cl_2$, or bromanilic, $H_2C_6O_4Br_2$, acids. Unfortunately, only a few single crystals of compound **2** could be obtained due to the unexpected and serendipitous presence of K^+ ions in this compound, caused by the presence of K^+ impurities in the recrystallization dmf solvent (as verified by ESI−mass spectrometry). Interestingly, attempts to prepare **2** using KOH instead of NaOH yield a monomeric compound formulated as $(PPh_3Et)_3[Fe(C_6O_4Cl_2)_3]$. As indicated in the Experimental Section, compound **4** is always obtained as a few single crystals mixed with a crystalline powder (**4′**) as a major phase. The unit cell obtained from the Pawley refinement of powder X-ray diffraction data of **4′** is consistent with those obtained for compounds **1** and **2** by single-crystal diffraction (see Supporting Information), suggesting that **4′** presents the same 2D structure as **1** and **2**. This is confirmed by the elemental analysis, which agrees with the formula $(NBu_3Me)_2[NaCr(C_6O_4Br_2)_3]$. The very small quantities obtained for compounds **2** and **4** (only a few single crystals) preclude a complete characterization of these two compounds and, therefore, only the structural analysis is presented here. Note that although their magnetic properties could not be measured, both compounds are expected to behave as compounds **1**, **3**, and **4′** because they all present well isolated Cr(III) or Fe(III) ions.

It is interesting to note that, although the five reported compounds have been prepared with a similar synthetic method, there are important modifications that lead to one or to another compound. Thus, compound **1**, a 2D structure with Na^+ in the layers and bulky PBu_3Me^+ cations between them is extracted with CH_2Cl_2, probably because the monomeric compound $(PBu_3Me)_3[Cr(C_6O_4Br_2)_3]$ is not extracted due to the lack of $\pi-\pi$ interactions between the cation and the anion. In contrast, in compound **2**, there are important $\pi-\pi$ cation−anion interactions that facilitate its extraction (as demonstrated by the fact that the organic phase yields the monomeric compound $(PPh_3Et)_3[Fe(C_6O_4Cl_2)_3]$). The aqueous phase must, therefore, contain very low amounts of $(PPh_3Et)^+$ cations and $[Fe(C_6O_4Cl_2)_3]^{3-}$ anions. The presence of low amounts of K^+ in the dmf solvent used for the recrystallization results in the formation of only a few crystals of compound **2**, that, in these conditions, must be less soluble than the $(PPh_3Et)_3[Fe(C_6O_4Cl_2)_3]$ monomer. Compound **3** is also obtained in an original way because the initial aqueous solution did not show any phase separation when CH_2Cl_2 was added. This fact has to be attributed to the smaller size of the NEt_3Me^+ cation (compared to all the other used cations). Compound **3** must be, therefore, the more stable and/or the less soluble in dmf of all the possible compounds that can originate from the mixture of solids. The presence of two Na^+ cations in **3** is not surprising because there were large amounts of Na^+ cations in the solution. The synthesis of compounds **4** and **4′** is more difficult to rationalize because the same synthesis gives rise to two polymorphs: the 2D honeycomb and the 3D (10,3) lattices. This is, as far as we know, the first time that these two polymorphs are obtained with oxalato or anilato and confirm the idea that both lattices are close in energy because both present the same number and types of bonds. Until now, all the known examples of isomeric 2D and 3D lattices (either homo- or heterometallic) had been obtained with different cations.

Crystal Structures. *Crystal Structures of $(PBu_3Me)_2[NaCr(C_6O_4Br_2)_3]$ (**1**) and $(PPh_3Et)_2[KFe(C_6O_4Cl_2)_3](dmf)_2$ (**2**).* These compounds present very similar crystal structures formed by cationic and anionic layers alternating along the [101] direction (Figure 1a) with interlayer separations of 8.869 Å in **1** and 9.414 Å in **2**. The anionic layer, formulated as $[M^IM^{III}(C_6O_4X_2)_3]^{2-}$ with $M^I/M^{III}/X$ = Na/Cr/Br (**1**) and K/Fe/Cl (**2**), shows the well-known honeycomb 2D structure where M^I and M^{III} ions are connected through $(C_6O_4X_2)^{2-}$ bridging ligands and occupy alternating vertices of the hexagons (Figure 1b). Each M^I ion is connected to three M^{III} ions through three anilato-type bridges and vice versa. In both compounds, the M^I and the M^{III} ions are perfectly located and do not present any disorder.

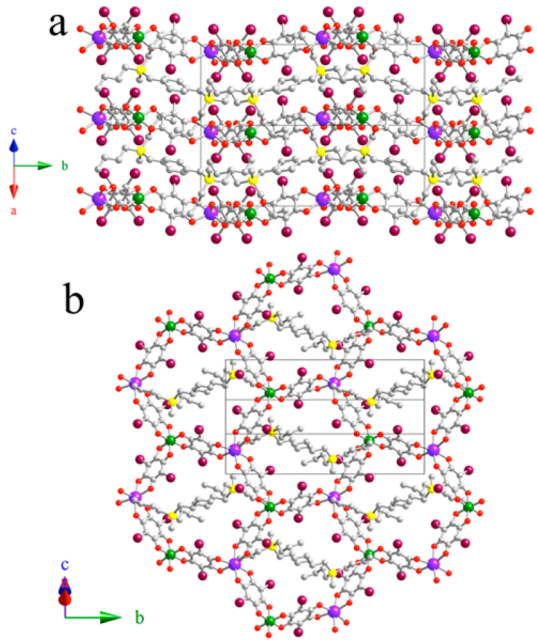

Figure 1. Structure of compound **1** (similar to **2**). (a) View of the alternating anion/cation layers. (b) View of the hexagonal honeycomb layer with the $(PBu_3Me)^+$ cations in the hexagons. Color code: Cr = green, Na = violet, O = red, C = gray, Br = brown, and *P* = yellow. H atoms have been omitted for clarity.

The cationic layer contains bulky $(PBu_3Me)^+$ or $(PPh_3Et)^+$ cations (in **1** and **2**, respectively) located above and below the hexagons of the anionic layers. In both compounds, one of the larger groups of the cations (butyl group in **1**, phenyl group in **2**) are inserted inside the hexagons, whereas the remaining groups are located between the layers (Figure 1a). The phenyl ring inserted in the anionic layer in compound **2** presents a

DOI: 10.1021/acs.inorgchem.5b00451
Inorg. Chem. 2015, 54, 5410−5418

$\pi-\pi$ interaction with one anilato ring (interplanar distance of 3.299 Å, Figure 2a). In **2**, there are two solvent dmf molecules located inside the hexagons (Figure 2a).

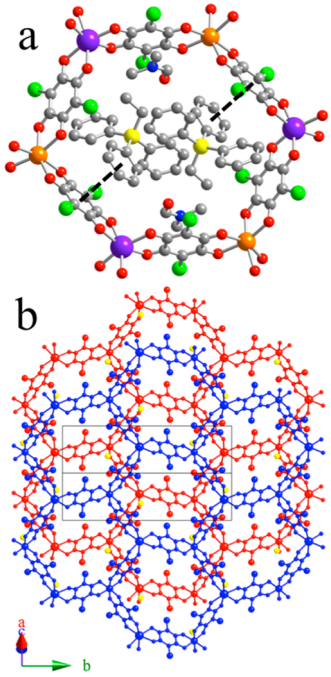

Figure 2. Structure of compound **2**. (a) View of the two dmf molecules and $(PPh_3Et)^+$ cations located in each hexagon showing the $\pi-\pi$ interactions between the phenyl and the anilato rings (dotted lines). (b) View of two consecutive anionic layer in **2** showing the alternating disposition. Color code in (a): Fe = orange, K = violet, O = red, C = gray, Cl = green, *N* = blue and *P* = yellow. H atoms have been omitted for clarity.

This structure resembles the one observed in the closely related $[M^{II}M^{III}(C_6O_4X_2)_3]^-$ compounds,[52] although there are some important differences: (i) in the $M^{II}M^{III}$ layers with the cation $[(H_3O)(phez)_3]^+$ (phez = phenazine), the M^{II} ions have a water molecule connected (or close) to the M^{II} ion, (ii) the charge in the $M^{II}M^{III}$ layers is −1 per hexagon compared to −2 in compounds **1** and **2**, and (iii) the $M^{II}M^{III}$ layers are eclipsed when the cation is $[(H_3O)(phez)_3]^+$ whereas they are alternated in compounds **1** and **2** (Figure 2b). Note that in the $[MnCr(C_6O_4X_2)_3]^-$ layers[52] prepared with $(NBu_4)^+$ and with four spin crossover cations,[53] the layers are also alternated.

It is to be noted that in the oxalato-based family, among the more than 100 reported structures of the type $[MM'(C_2O_4)_3]^{n-}$, there are only five examples[37−40] of the type $[NaCr(C_2O_4)_3]^{2-}$, only one[41] of the type $[NaFe(C_2O_4)_3]^{2-}$ and one[42] of the type $[KFe(C_2O_4)_3]^{2-}$. In the five examples of $[NaCr(C_2O_4)_3]^{2-}$ layers, the cations are either partially oxidized planar BEDT-TTF$^{+2/3}$ molecules (located perpendicular to the anionic layers)[37,39,41] or dications as $[Mg(H_2O)_6]^{2+}$,[38] $[Ni(cyclam)]^{2+}$, and $[Cu(tren)(H_2O)]^{2+}$.[40] The only reported examples of $[NaFe(C_2O_4)_3]^{2-}$ and $[KFe(C_2O_4)_3]^{2-}$ layers contains partially oxidized BEDT-TTF$^{+0.5}$ cations located perpendicular to the anionic layers.[41,42] In none of these seven examples are the cationic and anionic layers interpenetrated as observed in **1** and **2**. The smaller size of the oxalato-based hexagons (which are half the anilato-based ones) may be the reason for this lack of interpenetration in the oxalato family in contrast with the anilato one.

*Crystal Structure of $(NEt_3Me)[Na(dmf)][NaFe(C_6O_4Cl_2)_3]$ (**3**).* This compound presents a very original 3D structure that can be described as honeycomb $[NaFe(C_6O_4Cl_2)_3]^{2-}$ layers (Figure 3a) connected through interlayer Na^+ cations (Na2).

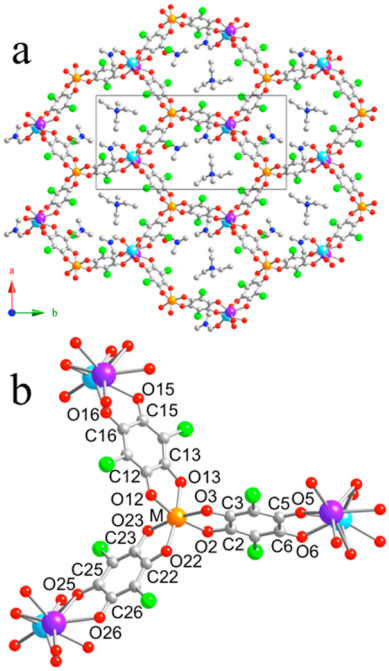

Figure 3. Structure of compound **3**. (a) View of one honeycomb layer with one $(NEt_3Me)^+$ cation per hexagon. (b) Labeling scheme of the coordination environment of the Fe(III) center and the three pairs of Na^+ ions connected to it. Color code: Fe = orange, Na1 = violet, Na2 = light blue, O = red, C = gray, Cl = green and *N* = blue. H atoms have been omitted for clarity.

The hexagonal layers present a structure similar to those of **1** and **2** (although not identical), where each Fe(III) ion is connected to the Na^+ atoms through three anilato bridges and vice versa (Figure 3b).

The most important difference is that in **3** additional Na^+ ions are located in between the anionic layers (blue Na^+ in Figure 4a). These Na^+ ions (Na2) connect both layers through several Na−O bonds connecting anilato ligands of both layers (Figure 4a). Thus, two of the three anilato ligands chelate the intralayer Na^+ ion (Na1) and at the same time are coordinated to the interlayer Na^+ (Na2) ion ($1\kappa^2O,O';2\kappa O$). The third anilato ligand is coordinated to two intralayer Na^+ (Na1) ions from the upper and lower layers and at the same time chelates the interlayer Na^+ (Na2) ion ($1\kappa O;2\kappa^2O,O';3\kappa O'$). This coordination modes give rise to the formation of chains of Na^+ dimers (Figure 4b), where each Na^+ ion is coordinated to four anilate ligands although with slight differences. Thus, the intralayer Na^+ (Na1) is coordinated to two chelating and two monodentate anilato ligands (total coordination number of 6), whereas the interlayer Na^+ (Na2) is coordinated to one chelating and three monodentate anilato ligands. The sixth coordination position of this Na2 ion is completed by a dmf molecule (Figure 4b).

The coordination geometry around the Na^+ ions can be described as distorted octahedra sharing a face (Figure 4b). If we consider that such a Na^+ dimer constitutes one vertex of the hexagon with the Fe(III) ion in the other, then the structure of **3** can be simply described as connected hexagonal layers of the

DOI: 10.1021/acs.inorgchem.5b00451
Inorg. Chem. 2015, 54, 5410−5418

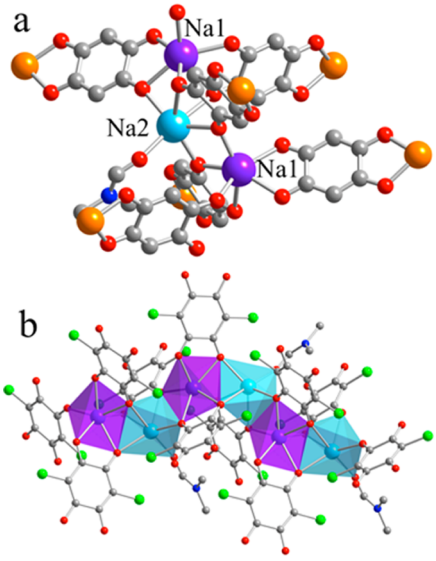

Figure 4. Structure of compound **3**. (a) View of two adjacent layers showing the interlayer Na2 cation (light blue) connecting both anionic layers (Cl atoms have been omitted for clarity). (b) View of a fragment of the chain of Na^+ cations showing the coordination modes of the chloranilate and dmf ligands. Color code: Na1 = light blue, Na2 = violet, O = red, C = gray, Cl = green and *N* = blue. H atoms have been omitted for clarity.

type $[Na_2Fe(C_6O_4Cl_2)_3]^-$ (Figure 5) with $(NEt_3Me)^+$ cations located in the hexagons (Figure 3a). The hexagonal layers are

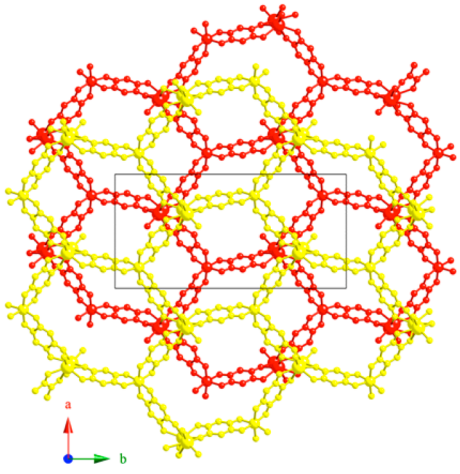

Figure 5. View of two adjacent layers in compound **3** showing the positions of the Fe(III) centers and the Na_2 dimers. H and Cl atoms have been omitted for clarity.

alternated in such a way that the Fe(III) ions of one layer are located above and below the centers of the hexagons of the neighboring layers, as can be observed in Figure 5. As far as we know, this is the first structure of this type described for any compound with oxalato or anilato-type ligands.

Crystal Structure of $(NBu_3Me)_2[NaCr(C_6O_4Br_2)_3]$ (4). This compound presents a 3D structure formed by two interlocked 3D (10,3) lattices (Figure 6). Each lattice is formed by the union of $[Cr(C_6O_4Br_2)_3]^{3-}$ units with Na^+ cations that alternate along the lattice and present the same chirality. Each Cr(III) ion is, therefore, connected to three different Na^+ ions by three bridging bromanilate ligands and vice versa,

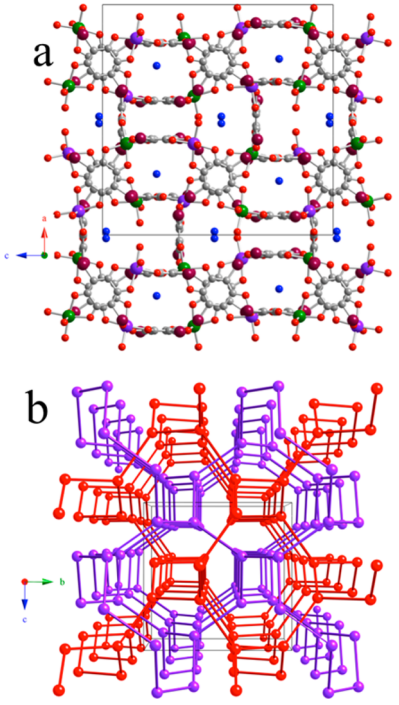

Figure 6. (a) View of the structure of compound **4** along the *b* direction. (b) Perspective view of the positions of the metal atoms in both interpenetrated sublattices (red and violet). Color code in (a): Cr = green, Na = violet, O = red, C = gray, Br = brown, and *N* = blue. H and C atoms of the cations have been omitted for clarity.

although the metal ions are disordered and each metal position contains both metal ions (Cr/Na) with 50% occupancy factor each. In this way, each metal ion appears as tris-chelated with a D_3 local symmetry. Because all the metal centers present the same chirality, the structure is formed by nonplanar 10-membered rings where each vertex is connected to three metals in a 3D (10,3) lattice. Although each of the two interpenetrated lattices is chiral, they present opposite chiralities, giving rise to an achiral 3D structure based on chiral lattices. This structure is similar to the one recently reported for the homometallic compounds $[NBu_4]_2[M^{II}_2(dhbq)_3]$ (M^{II} = Mn, Fe, Ni, Co, Zn and Cd) (dhbq = 2,5-dihydroxibenzoquinone = $C_6O_4H_2^{2-}$) and $[NBu_4]_2[Mn_2(C_6O_4Cl_2)_3]$[51] and to the 3D oxalato-based (10,3) lattices.[46,54] The $(NBu_3Me)^+$ cations are located in the cavities left by the two interpenetrated lattices (Figure 6a) with a shortest N−N distance of 9.71 Å.

Interestingly, in compounds **1** and **4**, the anionic lattices are isomeric $[NaCr(C_6O_4Br_2)_3]^{2-}$ and the cations are almost identical $(PBu_3Me)^+$ in **1** and $(NBu_3Me)^+$ in **4**. It is surprising that a simple change of a P by a N atom in the center of the bulk cation may lead to such a drastic change in the structure, even if for $(NBu_3Me)^+$ **4** is not the more stable phase as it appears as a minor one. To elucidate and optimize the synthesis of the 2D and 3D lattices, we are now investigating the role played by the synthetic conditions and the bulky cations in the final structure. In fact, as already mentioned, **4** crystallizes with a major phase (**4′**) that corresponds to the 2D structure observed in **1**, as deduced from powder X-ray data (see Supporting Information). This finding suggests that the 2D and 3D polymorphs are very close in energy, being the 2D phase slightly more stable and, therefore, the major one. In the analogous oxalate system, the 3D (10,3) structure is typically obtained with the use of chiral templating cations such as

DOI: 10.1021/acs.inorgchem.5b00451
Inorg. Chem. 2015, 54, 5410−5418

$[M(L)_3]^{n+}$ (L = bidentate ligand as bpy, ppy, phen,...).[46] In contrast, compound **4** gives rise to a double interpenetrated 3D (10,3) lattice even if the cation $(NBu_3Me)^+$ has no D_3 symmetry nor is chiral. Although very scarce, there are also some examples of oxalato-based (10,3) lattices prepared with achiral cations,[55−59] including the closely related compound $(PPh_3Me)_2[NaCr(C_2O_4)_3]$.[54] This compound (the only 3D oxalato-based lattice with a monocation) has the same cation as **1** and presents the same anionic lattice than **4** (although with oxalato instead of bromanilato).

The M^{III}−O bond distances in the $[M^{III}(C_6O_4X_2)_3]^{3-}$ units in **1**−**3** (Table 2) are similar to those observed in the few examples of monomeric $[M^{III}(C_6O_4X_2)_3]^{3-}$ units reported to date.[60−64] Compound **4** shows a much longer average Cr−O bond distance (2.154 Å) than compound **1** (1.967 Å) because in compound **4** the M positions correspond to a 50/50 mixture of Cr and Na ions (and the Na−O bond distances are ca. 2.3 Å in **1** and **3**). The intraligand C−C and C−O bond lengths of the side of the anilato ligand coordinated to the M^{III} ions vary significantly when compared with the typical C−O and C−C values for terminal anilato ligands. Thus, the C−O bond distances increase from 1.20 to 1.25 Å, when the O atoms are terminal, to 1.26−1.30 Å in **1**−**4** (Table 2). The corresponding OC−CO bond distance decreases from 1.53−1.60 Å to 1.51−1.54 Å in **1**−**4** because it partially loses its single-bond character (Table 2). In contrast, the C−O and C−C bond distances of the side of the anilato ligand coordinated to the alkali ions do not show any important variation (the C−O bonds are in the range 1.22−1.24 Å and the C−C bonds in the range 1.55−1.57 Å) (Table 2). This fact agrees with the weaker coordination of the anilato ligand to the alkaline ions (as shown by the longer M^I−O bond distances of ca. 2.3 Å in compounds **1**−**3**).

Table 2. Main Bond Lengths (Å) in the Anilate Ligands and around the M(III) Centres in 1−4 (Labelling Scheme in Figure 3b)

atoms	**1** (Cr)	**2** (Fe)	**3** (Fe)	**4** (Cr)
M−O2	1.976(3)	2.058(3)	2.0137(16)	2.170(7)
M−O3	1.970(3)	2.087(3)	2.0118(16)	2.138(7)
M−O12	1.956(3)	2.050(3)	2.0052(16)	2.170(7)
M−O13	1.963(3)	2.080(4)	2.0076(15)	2.138(7)
M−O22	1.972(3)	2.019(4)	2.0390(16)	2.170(7)
M−O23	1.966(3)	2.030(4)	1.9876(16)	2.138(7)
C2−O2	1.283(5)	1.268(6)	1.279(3)	1.256(10)
C3−O3	1.288(5)	1.284(5)	1.282(3)	1.263(11)
C5−O5	1.223(5)	1.242(6)	1.235(3)	1.256(10)
C6−O6	1.225(5)	1.224(5)	1.235(3)	1.263(11)
C12−O12	1.300(5)	1.266(6)	1.286(3)	1.256(10)
C13−O13	1.295(5)	1.287(6)	1.282(3)	1.263(11)
C15−O15	1.230(5)	1.235(6)	1.236(3)	1.256(10)
C16−O16	1.224(5)	1.236(5)	1.229(3)	1.263(11)
C22−O22	1.289(5)	1.275(7)	1.280(3)	1.256(10)
C23−O23	1.288(5)	1.294(6)	1.285(3)	1.263(11)
C25−O25	1.216(5)	1.231(6)	1.229(3)	1.256(10)
C26−O26	1.224(5)	1.250(6)	1.237(3)	1.263(11)
C2−C3	1.514(6)	1.525(6)	1.516(3)	1.572(12)
C5−C6	1.567(5)	1.562(6)	1.552(3)	1.572(12)
C12−C13	1.527(6)	1.531(6)	1.516(3)	1.572(12)
C15−C16	1.564(6)	1.548(6)	1.554(3)	1.572(12)
C22−C23	1.517(6)	1.542(6)	1.519(3)	1.572(12)
C25−C26	1.565(6)	1.565(7)	1.559(3)	1.572(12)

Magnetic Properties. As only a few single crystals of compounds **2** and **4** could be obtained, we have only performed magnetic measurements of the two compounds obtained as single pure phases (**1** and **3**), as confirmed by the powder X-ray diffraction (see Supporting Information) and on **4′**, the 2D major phase obtained in the synthesis of **4**. The product of the molar magnetic susceptibility per formula unit times the temperature ($\chi_m T$) for the Cr(III)-containing compounds (**1** and **4′**) show values of ca. 1.9 cm^3 K mol^{-1} at room temperatures, suggesting the presence of isolated S = 3/2 Cr(III) ions with $g \approx 2$, as observed in the structure of these compounds. When the samples are cooled, $\chi_m T$ remains constant down to very low temperature, where it shows a sharp decrease to reach a value of ca. 1.75 cm^3 K mol^{-1} at 2 K in both compounds (Figure 7a). This sharp decrease suggests the presence in **1** and **4′** of a zero field splitting (ZFS) of the S = 3/2 ground spin sate. The Fe(III)-containing compound (**3**) shows at room temperature a $\chi_m T$ value of ca. 4.44 cm^3 K mol^{-1} that remains constant when the sample is cooled. At very low temperatures, it shows a sharp decrease to reach a value of ca. 4.32 cm^3 K mol^{-1} at 2 K (Figure 7b). This behavior suggests the presence in **3** of isolated high spin S = 5/2 Fe(III) ions with a ZFS of the S = 5/2 ground spin state, in agreement with the structural results.

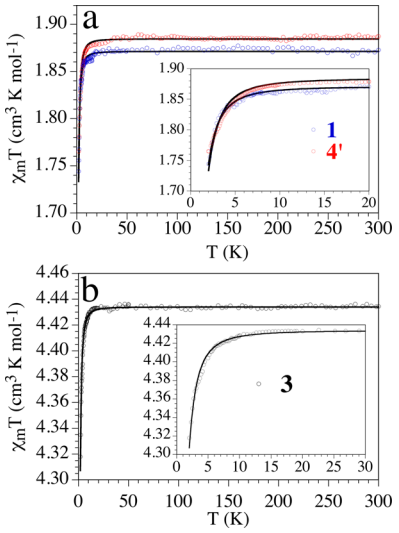

Figure 7. Thermal variation of $\chi_m T$ for (a) the Cr(III) compounds **1** and **4′** and (b) the Fe(III) compound **3**. Solid lines are the best fit to the isolated monomer models with zero field splitting (see text). Inset: low temperature regions.

Because the Na^+ cations are diamagnetic and are not expected to give rise to any magnetic coupling, compounds **1**, **3**, and **4′** can be considered from the magnetic point of view as being formed by isolated $[M^{III}(C_6O_4X_2)_3]^{3-}$ units. Accordingly, we have fit the magnetic properties of compounds **1**, **3**, and **4′** with simple models for isolated S = 3/2 (for **1** and **4′**) and S = 5/2 (for **3**) ions with ZFS.[65] These models reproduce very satisfactorily the magnetic properties of the three compounds in the whole temperature range with g = 1.998 and $|D|$ = 1.11 cm^{-1} for **1**, g = 2.005 and $|D|$ = 1.24 cm^{-1} for **4′**, and g = 2.013 and $|D|$ = 0.46 cm^{-1} for **3** (solid lines in Figure 7). Note that the sign of the zero field splitting parameter cannot be determined from powder susceptibility measurements and that we cannot discard the presence of a very weak antiferromag-

DOI: 10.1021/acs.inorgchem.5b00451
Inorg. Chem. 2015, 54, 5410−5418

netic contribution in the D parameter. These g and $|D|$ values are similar to those reported for the related isolated $[M^{III}(C_6O_4X_2)_3]^{3-}$ monomers,[62−64] in agreement with their resemblance from the magnetic point of view. The paramagnetic nature of compounds **1**, **3**, and **4′** is confirmed by the isothermal magnetizations at 2 K that can be well reproduced with a simple Brillouin function for S = 3/2 (for **1** and **4′**) and 5/2 (for **3**) with g values very close to 2 (see Supporting Information).

CONCLUSIONS

We have shown that the ability of anilato-type ligands to coordinate two different metals in a bis-bidentate mode (as oxalato does) can be exploited to build heterometallic anilato-based materials. Thus, we have prepared for the first time heterometallic honeycomb M(I)M(III) 2D lattices (**1**, **2**, and **4′**) as well as the first heterometallic 3D (10,3) anilate-based lattice (**4**). Compounds **4** and **4′** constitute the first example of 2D/3D polymorphs in the anilato-based family and has no precedent in the oxalato-based one. Furthermore, we have also prepared an unprecedented 3D structure formed by interconnected hexagonal honeycomb 2D lattices (**3**). Compounds **1**, **2**, **4**, and **4′** can be formulated as $A_2[M^IM^{III}(C_6O_4X_2)_3]$, where A is a bulky cation (PBu_3Me^+, PPh_3Et^+, or NBu_3Me^+), M^I is an alkaline metal (Na^+ or K^+), M^{III} is a transition metal (Cr or Fe), and X is an halogen (X = Cl or Br). The original structure of compound **3** shows the ability of the anilato-type ligands to simultaneously act as monodentate and chelate, bis-chelate, or even bis-monodentate and chelate. The use of this ability is expected to lead to novel polymeric magnetic structures using magnetic M^{II} and M^{III} ions. Studies in this direction are under way. On the other hand, the preparation of compound **4**, the first heterometallic 3D anilato-based lattice, constitutes a step forward in the preparation of the desired 3D heterometallic $M^{II}M^{III}$ lattices where long-range ferrimagnetic ordering is expected to occur, as was observed in the oxalato-based lattices.[46]

In summary, the five compounds here reported confirm the feasibility of the anilato-type ligands to be used as molecular bricks for the construction of a plethora of new molecular materials with extended structures and interesting magnetic properties, as was done with the oxalato ligand in the last two decades. Furthermore, anilato-based ligands present some important advantages: (i) they are bigger than oxalato and give rise to structures with much larger voids (twice in surface and almost three times larger in volume) where many different cations and solvent molecules can be incorporated, (ii) anilato-based ligand are easy to modify by changing the X group, leading to a fine-tuning of the magnetic coupling and also of the size and hydrophobicity of the cavities, and (iii) the X groups may also constitute the active centers of the cavities, allowing for an easy control of the affinities of these cavities toward different guest molecules.

ASSOCIATED CONTENT

Supporting Information

Plots with the observed and calculated profiles and difference plots of the Pawley refinements for compounds **1**, **3**, and **4′**; IR spectra of compounds **1**−**3** and **4′** and a table with the main IR frequencies and their assignments; isothermal magnetization plots at 2 K with the fit to the Brillouin function for compounds **1**, **3**, and **4′** (PDF, CIF). CCDC 1032217−1032220 (**1**−**4**, respectively) contains the supplementary crystallographic data for this paper. These data can be obtained free of charge from The Cambridge Crystallographic Data Centre via www.ccdc.cam.ac.uk/data_request/cif. The Supporting Information is available free of charge on the ACS Publications website at DOI: 10.1021/acs.inorgchem.5b00451.

AUTHOR INFORMATION

Corresponding Authors

*For S.B.: E-mail, sam.ben@uv.es.
*For C.J.G.G.: E-mail, carlos.gomez@uv.es.

Notes

The authors declare no competing financial interest.

ACKNOWLEDGMENTS

We thank the Spanish MINECO (projects CTQ-2011-26507 and CTQ-2014-59209-P) and the Generalitat Valenciana (projects PrometeoII/2014/076 and ISIC) for financial support. G.M.E. thanks the Spanish MINECO for a Ramón y Cajal contract.

REFERENCES

(1) Miller, J. S.; Gatteschi, D. *Chem. Soc. Rev.* **2011**, *40*, 3065−3066.
(2) Halcrow, M. A. *Chem. Soc. Rev.* **2011**, *40*, 4119−4142.
(3) Williams, J. M.; Ferraro, J. R.; Thorn, R. J.; Carlson, K. D.; Geiser, U.; Wang, H. H.; Kini, A. M.; Whangbo, M. H. In *Organic Superconductors (Including Fullerenes), Synthesis, Structure, Properties and Theory*; Crimes, R. N., Ed.; Prentice Hall: Englewood Cliffs, NJ, 1992.
(4) Glaser, T. *Chem. Commun.* **2011**, *47*, 116−130.
(5) Zhou, H.; Long, J. R.; Yaghi, O. M. *Chem. Rev.* **2012**, *112*, 673−674.
(6) Coronado, E.; Galan-Mascaros, J. R.; Gómez-García, C. J.; Laukhin, V. *Nature* **2000**, *408*, 447−449.
(7) Graham, A. W.; Kurmoo, M.; Day, P. *J. Chem. Soc., Chem. Commun.* **1995**, 2061−2062.
(8) Coronado, E.; Gómez-García, C. J.; Nuez, A.; Romero, F. M.; Waerenborgh, J. C. *Chem. Mater.* **2006**, *18*, 2670−2681.
(9) Coronado, E.; Gómez-García, C. J.; Nuez, A.; Romero, F. M.; Rusanov, E.; Stoeckli-Evans, H. *Inorg. Chem.* **2002**, *41*, 4615−4617.
(10) Pop, F.; Auban-Senzier, P.; Canadell, E.; Rikken, G. L.; Avarvari, N. *Nature Commun.* **2014**, *5*, 3757.
(11) Riobe, F.; Piron, F.; Rethore, C.; Madalan, A. M.; Gómez-García, C. J.; Lacour, J.; Wallis, J. D.; Avarvari, N. *New J. Chem.* **2011**, *35*, 2279−2286.
(12) Coronado, E.; Minguez Espallargas, G. *Chem. Soc. Rev.* **2013**, *42*, 1525−1539.
(13) Kurmoo, M. *Chem. Soc. Rev.* **2009**, *38*, 1353−1379.
(14) Clemente-León, M.; Coronado, E.; Gómez-García, C. J.; López-Jordà, M.; Camón, A.; Repollés, A.; Luis, F. *Chem.—Eur. J.* **2014**, *20*, 1669−1676.
(15) Adhikary, C.; Koner, S. *Coord. Chem. Rev.* **2010**, *254*, 2933−2958.
(16) Escuer, A.; Esteban, J.; Perlepes, S. P.; Stamatatos, T. C. *Coord. Chem. Rev.* **2014**, *275*, 87−129.
(17) Newton, G. N.; Nihei, M.; Oshio, H. *Eur. J. Inorg. Chem.* **2011**, *2011*, 3031−3042.
(18) Biswas, S.; Gómez-García, C. J.; Clemente-Juan, J. M.; Benmansour, S.; Ghosh, A. *Inorg. Chem.* **2014**, *53*, 2441−2449.
(19) Batten, S. R.; Murray, K. S. *Coord. Chem. Rev.* **2003**, *246*, 103−130.
(20) Tamaki, H.; Zhong, Z. J.; Matsumoto, N.; Kida, S.; Koikawa, M.; Achiwa, N.; Hashimoto, Y.; Okawa, H. *J. Am. Chem. Soc.* **1992**, *114*, 6974−6979.
(21) Atovmyan, L. O.; Shilov, G. V.; Lyubovskaya, R. N.; Zhilyaeva, E. I.; Ovanesyan, N. S.; Pirumova, S. I.; Gusakovskaya, I. G.; Morozov, Y. G. *J. Exp. Theor. Phys. Lett.* **1993**, *58*, 766−769.

DOI: 10.1021/acs.inorgchem.5b00451
Inorg. Chem. 2015, 54, 5410−5418

(22) Mathoniere, C.; Nuttall, C. J.; Carling, S. G.; Day, P. *Inorg. Chem.* **1996**, *35*, 1201−1206.
(23) Alberola, A.; Coronado, E.; Galan-Mascaros, J. R.; Gimenez-Saiz, C.; Gómez-García, C. J. *J. Am. Chem. Soc.* **2003**, *125*, 10774−10775.
(24) Benard, S.; Riviere, E.; Yu, P.; Nakatani, K.; Delouis, J. F. *Chem. Mater.* **2001**, *13*, 159−162.
(25) Kida, N.; Hikita, M.; Kashima, I.; Okubo, M.; Itoi, M.; Enomoto, M.; Kato, K.; Takata, M.; Kojima, N. *J. Am. Chem. Soc.* **2008**, *131*, 212−220.
(26) Clemente-Leon, M.; Coronado, E.; Carmen Gimenez-Lopez, M.; Soriano-Portillo, A.; Waerenborgh, J. C.; Delgado, F. S.; Ruiz-Perez, C. *Inorg. Chem.* **2008**, *47*, 9111−9120.
(27) Clemente-Leon, M.; Coronado, E.; Lopez-Jorda, M.; Desplanches, C.; Asthana, S.; Wang, H.; Letard, J. *Chem. Sci.* **2011**, *2*, 1121−1127.
(28) Gruselle, M.; Train, C.; Boubekeur, K.; Gredin, P.; Ovanesyan, N. *Coord. Chem. Rev.* **2006**, *250*, 2491−2500.
(29) Train, C.; Gheorghe, R.; Krstic, V.; Chamoreau, L.; Ovanesyan, N. S.; Rikken, G. L. J. A.; Gruselle, M.; Verdaguer, M. *Nature Mater.* **2008**, *7*, 729−734.
(30) Okawa, H.; Shigematsu, A.; Sadakiyo, M.; Miyagawa, T.; Yoneda, K.; Ohba, M.; Kitagawa, H. *J. Am. Chem. Soc.* **2009**, *131*, 13516−13522.
(31) Clemente-Leon, M.; Coronado, E.; GalanMascaros, J. R.; Gómez-García, C. J. *Chem. Commun.* **1997**, 1727−1728.
(32) Coronado, E.; Clemente-León, M.; Galán-Mascarós, J. R.; Giménez-Saiz, C.; Gómez-García, C. J.; Martínez-Ferrero, E. *J. Chem. Soc., Dalton Trans.* **2000**, 3955−3961.
(33) Coronado, E.; Galán-Mascarós, J.; Gómez-García, C.; Ensling, J.; Gütlich, P. *Chem.—Eur. J.* **2000**, *6*, 552−563.
(34) Coronado, E.; Galan-Mascaros, J. R.; Gómez-García, C. J.; Martinez-Agudo, J. M. *Adv. Mater.* **1999**, *11*, 558−561.
(35) Coronado, E.; Galan-Mascaros, J. R.; Gómez-García, C. J.; Martinez-Agudo, J. M.; Martinez-Ferrero, E.; Waerenborgh, J. C.; Almeida, M. *J. Solid State Chem.* **2001**, *159*, 391−402.
(36) Bénard, S.; Yu, P.; Audière, J. P.; Rivière, E.; Clément, R.; Guilhem, J.; Tchertanov, L.; Nakatani, K. *J. Am. Chem. Soc.* **2000**, *122*, 9444−9454.
(37) Martin, L.; Day, P.; Horton, P.; Nakatsuji, S.; Yamada, J.; Akutsu, H. *J. Mater. Chem.* **2010**, *20*, 2738−2742.
(38) Suh, J. S.; Shin, J. Y.; Yoon, C.; Lee, K. W.; Suh, I. H.; Lee, J. H.; Ryu, B. Y.; Lim, S. S. *Bull. Korean Chem. Soc.* **1994**, *15*, 245−249.
(39) Martin, L.; Day, P.; Nakatsuji, S.; Yamada, J.; Akutsu, H.; Horton, P. *CrystEngComm* **2010**, *12*, 1369−1372.
(40) Suh, M. P.; Jeon, J. W.; Moon, H. R.; Min, K. S.; Choi, H. J. *C. R. Chim.* **2005**, *8*, 1543−1551.
(41) Kurmoo, M.; Graham, A. W.; Day, P.; Coles, S. J.; Hursthouse, M. B.; Caulfield, J. L.; Singleton, J.; Pratt, F. L.; Hayes, W. *J. Am. Chem. Soc.* **1995**, *117*, 12209−12217.
(42) Coronado, E.; Curreli, S.; Gimenez-Saiz, C.; Gómez-García, C. J. *Inorg. Chem.* **2012**, *51*, 1111−1126.
(43) Coronado, E.; Curreli, S.; Gimenez-Saiz, C.; Gómez-García, C. J. *J. Mater. Chem.* **2005**, *15*, 1429−1436.
(44) Butler, K. R.; Snow, M. R. *J. Chem. Soc. A* **1971**, 565−569.
(45) Decurtins, S.; Schmalle, H. W.; Schneuwly, P.; Ensling, J.; Guetlich, P. *J. Am. Chem. Soc.* **1994**, *116*, 9521−9528.
(46) Coronado, E.; Galan-Mascaros, J. R.; Gómez-García, C. J.; Martinez-Agudo, J. M. *Inorg. Chem.* **2001**, *40*, 113−120.
(47) Kitagawa, S.; Kawata, S. *Coord. Chem. Rev.* **2002**, *224*, 11−34.
(48) Luo, T.; Liu, Y.; Tsai, H.; Su, C.; Ueng, C.; Lu, K. *Eur. J. Inorg. Chem.* **2004**, 4253−4258.
(49) Abrahams, B. F.; Coleiro, J.; Ha, K.; Hoskins, B. F.; Orchard, S. D.; Robson, R. *J. Chem. Soc., Dalton Trans.* **2002**, 1586−1594.
(50) Shilov, G. V.; Nikitina, Z. K.; Ovanesyan, N. S.; Aldoshin, S. M.; Makhaev, V. D. *Russ. Chem. Bull.* **2011**, *60*, 1209−1219.
(51) Abrahams, B. F.; Hudson, T. A.; McCormick, L. J.; Robson, R. *Cryst. Growth Des.* **2011**, *11*, 2717−2720.
(52) Atzori, M.; Benmansour, S.; Mínguez Espallargas, G.; Clemente-León, M.; Abhervé, A.; Gómez-Claramunt, P.; Coronado, E.; Artizzu, F.; Sessini, E.; Deplano, P.; Serpe, A.; Mercuri, M. L.; Gómez García, C. J. *Inorg. Chem.* **2013**, *52*, 10031−10040.
(53) Abhervé, A.; Clemente-León, M.; Coronado, E.; Gómez-García, C. J.; Verneret, M. *Inorg. Chem.* **2014**, *53*, 12014−12026.
(54) M. Russell, V.; C. Craig, D.; L. Scudder, M.; G. Dance, I. *CrystEngComm* **2000**, *2*, 16−23.
(55) Clemente-Leon, M.; Coronado, E.; Lopez-Jorda, M. *Dalton Trans.* **2013**, *42*, 5100−5110.
(56) Clemente-León, M.; Coronado, E.; López-Jordá, M.; Waerenborgh, J. C. *Inorg. Chem.* **2011**, *50*, 9122−9130.
(57) Coronado, E.; Galán Mascarós, J. R.; Giménez-López, M. C.; Almeida, M.; Waerenborgh, J. C. *Polyhedron* **2007**, *26*, 1838−1844.
(58) Clemente-Leon, M.; Coronado, E.; Lopez-Jorda, M.; Minguez Espallargas, G.; Soriano-Portillo, A.; Waerenborgh, J. C. *Chem.—Eur. J.* **2010**, *16*, 2207−2219.
(59) Shen, H.; Bu, W.; Liao, D.; Jiang, Z.; Yan, S.; Wang, G. *Inorg. Chem.* **2000**, *39*, 2239−2242.
(60) Spengler, R.; Lange, J.; Zimmermann, H.; Burzlaff, H.; Veltsistas, P. G.; Karayannis, M. I. *Acta Crystallogr., Sect. B: Struct. Sci.* **1995**, *51*, 174−177.
(61) Min, K. S.; Rhinegold, A. L.; Miller, J. S. *J. Am. Chem. Soc.* **2006**, *128*, 40−41.
(62) Benmansour, S.; Coronado, E.; Giménez-Saiz, C.; Gómez-García, C. J.; Röβer, C. *Eur. J. Inorg. Chem.* **2014**, *2014*, 3949−3959.
(63) Atzori, M.; Artizzu, F.; Sessini, E.; Marchio, L.; Loche, D.; Serpe, A.; Deplano, P.; Concas, G.; Pop, F.; Avarvari, N.; Laura Mercuri, M. *Dalton Trans.* **2014**, *43*, 7006−7019.
(64) Atzori, M.; Pop, F.; Auban-Senzier, P.; Gómez-García, C. J.; Canadell, E.; Artizzu, F.; Serpe, A.; Deplano, P.; Avarvari, N.; Mercuri, M. L. *Inorg. Chem.* **2014**, *53*, 7028−7039.
(65) O'Connor, C. J. *Prog. Inorg. Chem.* **1982**, *29*, 203−283.
(66) Sheldrick, G. M. *Acta Crystallogr., Sect. A: Found. Crystallogr.* **2008**, *64*, 112−122.
(67) Pawley, G. S. *J. Appl. Crystallogr.* **1981**, *14*, 357−361.
(68) Coelho, A. A. *TOPAS*, version 4.1; Academic Press: New York, 2007; http://www.topas-academic.net.
(69) Bain, G. A.; Berry, J. F. *J. Chem. Educ.* **2008**, *85*, 532−536.

DOI: 10.1021/acs.inorgchem.5b00451
Inorg. Chem. 2015, 54, 5410−5418